Identifying coastal land cover types using a hybrid approach of optical and SAR satellite data in the Auckland region

B. M. Collings[1], M. R. Ford[1], M. E. Dickson[1]
School of Environment, University of Auckland, 23 Symonds St, Auckland, New Zealand.
email: ben.collings@auckland.ac.nz

Abstract
Satellite remote sensing provides low-cost data appropriate for assessing coastal change at large scales. To apply such techniques at regional and national scales, initial identification of coastal land cover types using satellite data is required with high degrees of accuracy. In New Zealand the physical diversity of the coast presents challenges for large-scale application of remote sensing techniques. This paper aims to identify coastal land cover types in the Auckland region by validating a hybrid rule-based and machine learning methodology developed in Google Earth Engine that utilises freely available satellite data from both optical and synthetic aperture radar (SAR) sensors. Data pre-processing was applied to develop a composite image for 2019 containing data from Sentinel-1 (SAR) and Sentinel-2 (optical) satellites. Hierarchal rules were developed to separate water and vegetation land covers. The remaining land cover types (titanomagnetite volcanic sand, quartz-feldspathic sand, intertidal, artificial surfaces, and rock coasts) were identified using a random forest machine learning classifier trained with high-resolution satellite data and ancillary datasets. The overall accuracy of the approach was 82% with a kappa statistic of 0.79. The overall detection of sandy coast in the Auckland region had a producer's accuracy of 93.6% and user's accuracy of 86.4%. SAR data provides valuable information about the physical/textural characteristics of built areas that reduces the misclassification of these areas as quartz-feldspathic sand, leading to greater accuracies compared to using just optical data. The methodology provides a low-cost solution for the identification of coastal landcover types that can be applied at national scale. Such information will be instrumental in efforts to develop remote sensing approaches to accurately detect coastal change beyond local scales.

Keywords: Remote sensing, Synthetic Aperture Radar, Optical, Google Earth Engine, classification.

1. Introduction

Depositional coastal environments are subject to a variety of hazards, particularly erosion and flooding which can occur at a range of temporal and spatial scales and are influenced by both environmental and anthropogenic factors [19]. Timing and magnitude of such hazards are poorly resolved and the impacts of climate change will contribute further, uncertainty, thus adaptation at the coast is a key global issue [12]. Between 2006 – 2015 rates of global mean sea level rise (MSLR) were greater by a factor of two compared with MSLR in the 20th century [17]. This acceleration is associated with anthropogenic warming [9] which is likely to exacerbate the impacts of coastal hazards. Effective strategic planning and mitigation therefore requires scientific information describing past, current, and future rates of coastal change at local, regional, and national scales.

Earth observation (EO) data has been widely applied to investigate coastal change by analysing shoreline position. Whilst commercial data can provide very high spatial resolution (< 1 m), many investigations have been driven by access to freely available EO imagery. Geographic coverage and temporal/spatial resolutions (5 – 16 days/10 – 30 m) offered by publicly available EO data (e.g., Landsat and Sentinel) can address limitations associated with traditional methods of monitoring shoreline position [1]. Several types of EO data have been used, including optical and Synthetic Aperture Radar (SAR). Passive optical sensors (Landsat/Sentinel-2) operate in the visible to infrared portion of the electromagnetic spectrum, capturing information, via solar radiation about the spectral characteristics of the Earth's surface that are reflected or emitted. SAR (Sentinel-1) are active sensors, transmitting and receiving energy in the microwave portion of the spectrum. Information is recorded as backscatter and interacts with the physical characteristics of surface features. Key benefits of SAR systems are that the signals penetrate clouds and are therefore not limited by weather. Both optical and SAR are effective at separating terrestrial and water features due to explicit variations in spectral and textural properties respectively.

Techniques tend to focus on the extraction of instantaneous waterlines (IW) as a proxy for shoreline position [1]. Alterations in the position of this boundary are considered a significant indicator of change and is frequently used by scientists. Information from shoreline positions analysis is required for coastal management, engineering/design of coastal protection, calibration/validation of modelling approaches and, assessments of coastal hazards and associated mitigating practises [1]. Techniques used to separate land and water in EO data provide objective and repeatable approaches to extract the IW shoreline with high degrees of accuracy [21]. The position of the IW is primarily a function of wave

and tidal processes and beach gradient. In some environments this can mean spatial/temporal variation can be tens to hundreds of metres at very short timescales. Whilst a simple indicator of change at the coast, interpreting the IW position and what this means in the context of long-term change for a given section of sandy coast is uncertain.

Pixel-based classification techniques are an effective low cost means of utilising EO data for the identification and monitoring of land cover/use. A plethora of applications have been developed and applied to monitor change for a range of land cover types (e.g., forestry, surface water, urban development) from regional to global scales [3]. This has been driven by the accessibility of appropriate data and improvements in computing performance, namely developments in cloud computing to process large quantities of data. Platforms such as Google Earth Engine (GEE) provide petabytes of freely available remote sensing datasets offering global coverage since the 1970s, as well as the tools and processing power to analyse the data from any computer with a good internet connection [10]. Pixel based classification presents the opportunity to leverage meaningful information from all pixels across the coastal zone.

Per-pixel processing techniques have been used in remote sensing coastal change investigations at regional and global scales but are limited compared to shoreline extraction applications. Classification techniques have been used to assess annual water frequency as a proxy for change [23]. The development of cloud computing platforms (e.g., GEE) has driven global scale analyses of the coast using per-pixel techniques, including supervised machine learning classification of the worlds' sandy beaches [15]. Supervised classification techniques have also been used to improve IW shoreline extraction techniques by removing noise associated with landcover types at the coast other than water and sand [21]. These approaches all focus on the separation of water and non-water pixels as an indicator of change. There is a lack of per-pixel techniques that consider information across the entire coastal zone.

For successful implementation of supervised classification algorithms training data must be fully representative of all thematic classes observed and therefore all training pixels must contribute to the spectral signature of a given class without contribution of mixed pixels [14]. The collection of appropriate training data is therefore paramount. The New Zealand coastline is highly dynamic and variable. Sediment type, for instance, can vary both regionally and locally, which is evident when comparing east and west coasts of both the North Island and South Island. The north-western coastlines are dominated by titanomagnetite sands, whilst on the east coast beaches are comprised of traditional quartz-feldspathic and carbonate sands [4]. Physical characteristics must be considered in classification workflows to develop robust products that can be used to identify change at a pixel level for a range of coastal land cover types. The aim of this study is the development of a per-pixel classification workflow using a hybrid rule-based, machine learning approach to identify coastal land cover types at the New Zealand coast that is scalable for the development of a national coastal land cover product. Such a product is the initial step in the development of a change detection workflow to assess past, current, and future change across coastal land cover types that can provide better proxies of change than the sole use of the shoreline position. In doing so, accounting for the dynamic coastal environments across New Zealand. The methodology was developed and validated for the Auckland region using all available data from Sentinel-1 and 2 for the year 2019 to develop a baseline coastal land cover product.

2. Methods

2.1 Study area and data

The Auckland region was selected as an appropriate study region as a wide range of coastal land cover and beach types are found across the Auckland region. All available images from Sentinel-1 (229 images) and Sentinel-2 with cloud cover < 20% (242 images) for the year of 2019 were used. The coastal region was defined by generating a 1500 m buffer around the mean high water (MHW) mark coastline available from Land Information New Zealand (LINZ), at a scale of 1:50,000. This provided a broad 3 km zone at the coast as the study area.

High resolution datasets from Planet's RapidEye (5 m) constellation were acquired for 2019 for the generation of reference data to train and validate classification outputs described in section 2.3. The focus of the study was the identification of depositional sediment in the coastal zone. The Shuttle Radar Topography Mission (STRM) elevation model [6] was used to define an elevation threshold of 10 m that removed most cliffed sections of coast. This is a freely available dataset with global coverage. Most datasets were available in GEE, having had necessary pre-processing steps applied they are considered analysis ready data (ARD). Sentinel-2 level-2A surface reflectance products and Sentinel-1 level-1 ground range detected (GRD) products were used in the classification workflow (Figure 1). Data processing was performed in the GEE code editor through a web-browser.

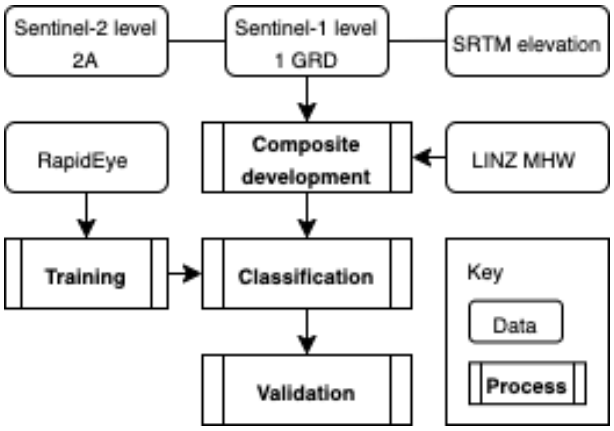

Figure 1 Workflow implemented in Google Earth Engine. All processing took place in the code editor. This provides functions to analyse EO data for large geographic areas efficiently.

Composite development

Multi-temporal composite images were derived using statistical aggregations of all available pixel values within the time period. Cloud masking was performed on optical data using the cloud mask provided with Sentinel-2 level 2A products. Several spectral indices (normalised difference vegetation index (NDVI) , normalised difference water index (NDWI) [8], modified normalised difference water index (MNDWI) [22] and automated water extraction index (AWEI) [7] for the identification of vegetation and water in EO data) were calculated for each optical image and composite bands were adapted from [16] (Table 2). To ensure that only cloud-free observations were included the 15th percentile pixel values were used for all optical bands. Cloudy pixels exhibit high spectral reflectance values, by selecting the 15th percentile value cloudy observations were excluded from the composite [11].

Table 1 Optical composite bands derived from the indices images adapted from [18]. These bands were passed to the machine learning classifier. This provided greater information for the separation of spectrally similar classes.

Indices Images	Composite bands
NDVI	Interval mean 10 – 90
NDWI, MNDWI, AWEI	Minimum
	Maximum
	Median
	Standard deviation
	10th percentile
	25th percentile
	50th percentile
	75th percentile
	90th percentile

SAR data is sensitive to acquisition parameters (e.g., incidence angle, polarisation) [20], so pre-processing steps were required. Incidence angle corrections were applied to remove observations with low/high angles. Sentinel-1 offers dual polarisation, transmitting and receiving in both vertical and horizontal planes. In this study, 12 mean SAR bands were derived. These were normalised by Sentinel-1 acquisition parameters (e.g., orbit and polarisation). Optical and SAR composites were stacked, creating an annual composite for 2019 with 51 bands. All bands were resampled to 20 m.

2.2 Classification

A supervised hierarchal classification workflow was devised utilising both rules and a random forest machine learning classifier [2] to separate coastal landcover into seven classes (Figure 2). Automated Otsu thresholding [18] was applied to median MNDWI to separate water and non-water pixels and then to interval mean NDVI to separate vegetation and non-vegetation classes. Remaining pixels were classified by the random forest classifier. One hundred training pixels per class were identified using high resolution optical imagery, to ensure that training pixels were fully representative of each given class and mixed pixels were excluded. Random forest was selected due to the ability of the algorithm to rank the importance of input variables to assess which bands that contribute most to the classification.

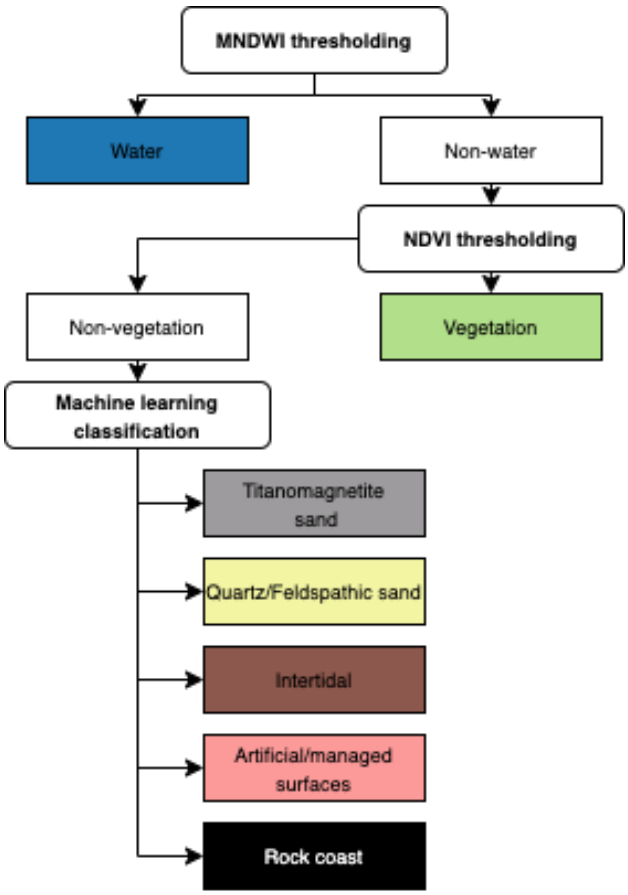

Figure 2 Class hierarchy implemented in the classification. The seven thematic classes are coloured. Water and vegetation were separated via initial rules and remaining classes were identified through machine learning.

2.3 Validation

A set of 250 points per class were generated using a stratified sampling approach and visually assessed against high resolution images acquired from the same period as the data input to the classification. Error matrices were derived to assess the accuracy of classification outputs. An error matrix was used to assess the relationship, on a class-by-class basis, between ground truth points and the classification output [13]. This allowed an evaluation of omission and commission errors. Omission errors represents pixels that should have been classified as a given class but have been excluded. Commission errors include pixels that are incorrectly classified as another class. Overall accuracy and kappa were calculated as well as User's (UA) and Producer's (PA) accuracy to assess the accuracy of individual classes. UA is associated with commission errors and specifies the probability that a pixel classified as a given class represents that class on the ground. PA represents how well training set pixels of a given class have been classified. Validation metrics for optical and optical/SAR classifications derived from the same training pixels and validated with the same subset of ground truth points were compared to evaluate the combination of optical and SAR data.

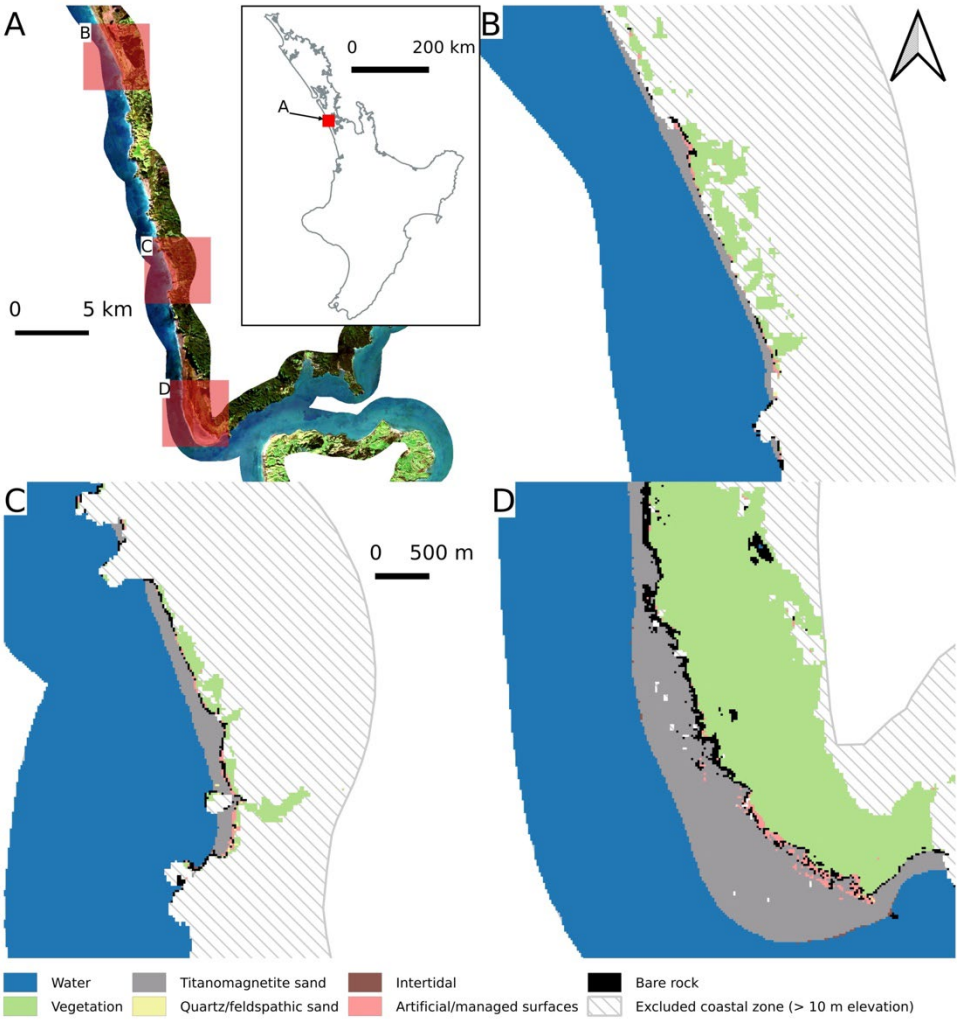

Figure 3 A. True colour image of the Sentinel-2 optical images used in the classification with examples of the classification output for B. Muriwai, C. Piha, D. Whatipu. Titanomagnetite was the most accurately classified depositional coastal land cover type. This highlights the strength of the workflow to detect coastal landcover on a per-pixel basis.

3. Results

Overall accuracy for the classification output utilising both composites was 82% (kappa 0.79). Accuracies between classes varied considerably, PA ranged from 75% – 100% and UA 57.2% - 97.2% (Table 3). Vegetation was the most accurately discriminated class. Combined accuracy for sandy coast was good (UA = 93.6% and PA = 86.4%). Titanomagnetite sand was most accurately classified which was particularly evident at locations along the west coast (Figure 3). Most misclassifications within the class were associated with quartz-feldspathic sand. The highest omission errors were for the water class (PA = 64.5%), associated with misclassification of pixels as intertidal and rock coast. This suggests that the initial rule separating land and water pixels is excluding water pixels, particularly at boundaries with bare rock and intertidal areas.

Table 2 User's and Producer's accuracy from the final classification output using optical and SAR data. Separation of depositional sediment was good. The results indicate the classification is effective at identifying coastal landcover in the Auckland region.

Class	Producer's (%)	User's (%)
Water	64.5	94.4
Vegetation	99.6	97.2
Titanomagnetite sand	92.4	88
Quartz-feldspathic sand	75	91.2
Intertidal	70.1	71.2
Rock coast	100	57.2
Artificial/managed surfaces	93	74.8

Omission errors for quartz-feldspathic sand were high (PA = 75%), primarily associated with pixels misclassified as artificial/managed surfaces. Rock coast was most poorly classified (UA = 57.2%) with very high commission errors associated with all other classes but contained no omission errors meaning all rock coast was correctly identified, but a high proportion of non-rock coast was incorrectly identified as rock. The intertidal class also performed poorly associated with misclassification of all other classes and commission errors related to the water class. A comparison of validation results between supervised classification outputs that used optical and both SAR and optical data found that using both datasets led to greater accuracies. Overall accuracy and kappa increased by 3.78% and 0.04 respectively. Accuracy for sandy coast classes using optical and SAR data increased both UA and PA by 5.8% and 10.7% respectively. Analysis of UA and PA showed increases in all classes, except for decreases in PA in the titanomagnetite sand class and UA for the intertidal class when using the combination of SAR and optical data (Figure 4). The most significant increases in UA and PA were found for the quartz-feldspathic sand class and rock coast class.

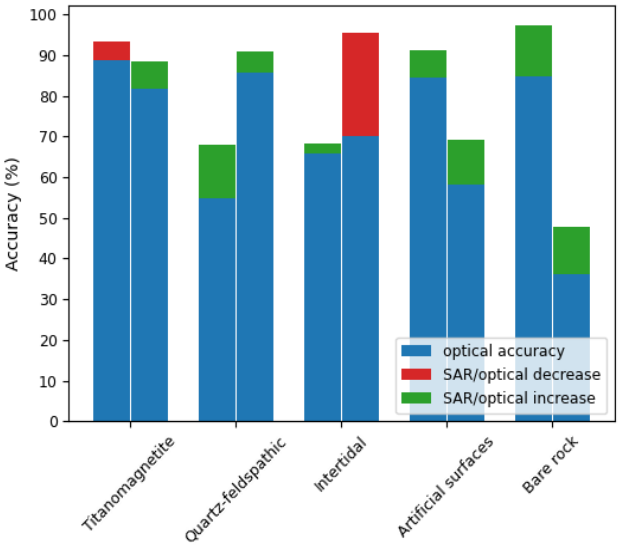

Figure 4 Stacked bar chart showing the increase in PA (left bar) and UA (right bar) for each class in the supervised classification respectively. Improvements were evident in all classes. Misclassification of Quartz-feldspathic sand as artificial/managed surfaces was reduced.

Increased PA associated with quartz-feldspathic sand (13.16%) were driven by improved separation of artificial/managed surface pixels. Improved accuracy for the bare rock class (PA: 12.58%, UA: 11.81%) was associated with reduced misclassification of all other classes, particularly water and titanomagnetite sand. In the artificial/managed surface class, successful identification of quartz-feldspathic sand pixels accounted for 88.7% of the reduction. A decrease in PA (-4.62%) was evident for titanomagnetite sand which was due to misclassification of pixels as rock coast. Decreases in UA (-25.39%) for the intertidal class were associated with the increased misclassification of water pixels. The hierarchal rules to separate water/non-water and vegetation/non-vegetation were highly accurate. It is also clear that a combination of optical and SAR data to train the random forest classifier produced a more accurate output compared to the use of optical data. The greatest reductions in error were associated with the improved separation of sandy coast, rock coast and urban areas.

4. Discussion

Using a combination of optical and SAR EO data a variety of coastal land cover types in the Auckland region have been accurately identified using GEE on a per-pixel basis at 20 m spatial resolution. The methodology developed is considered the first key step toward per-pixel change detection to assess coastal change at regional to national scales, providing information about a range of coastal landcover types rather than a shoreline-based approach. Previous approaches implementing pixel-based analyses have either focused on the separation of land and water [15], [23], or the identification of land cover types to reduce noise and improve the extraction of IW shorelines [21]. Whilst these techniques provide robust repeatable approaches to analyse rates of change of the IW shoreline position, important information captured by EO data could be removed. A benefit of pixel-based techniques is the ability to assess change on a per-pixel basis across the entire coastal zone rather than condensing information to focus on a single shoreline proxy.

Through the identification of a range of land cover types in the coastal zone, better understanding of the impacts of coastal hazards can be investigated through the response of individual landcover types rather than the response of the shoreline position. For example, the hierarchal rules accurately discriminate water and vegetation with the highest UA values for those classes. Vegetation was the most accurate class. Further separation of the class could provide information about specific coastal/marine vegetation (e.g., Mangrove and dune vegetation) for New Zealand's coast to better understand the impact of vegetation at the coast.

A major benefit of this workflow can be implemented with EO data from multiple sensors and time instances. The Landsat archive contains historical data from the last four decades. Applying this methodology to multiple years utilising both Sentinel and Landsat sensors could provide a long-term national scale assessment of New Zealand's coast.

4.1 Improvements from SAR

Incorporating SAR data in the classification led to increases in accuracy, most notably, improved detection of sandy coast. SAR data was combined with optical data to provide information about the physical properties if the land cover types under investigation to the machine learning classifier. Confusion between artificial/managed surfaces and quartz-feldspathic sand is evident in optical data as spectral characteristics are similar [13]. SAR interreacts with the physical characteristics of land cover surfaces providing contextual information which is useful for the detection of anthropogenic surfaces and separation of quartz-feldspathic sand, especially in developed coastal areas where infrastructure is within close proximity of beaches (Figure 5).

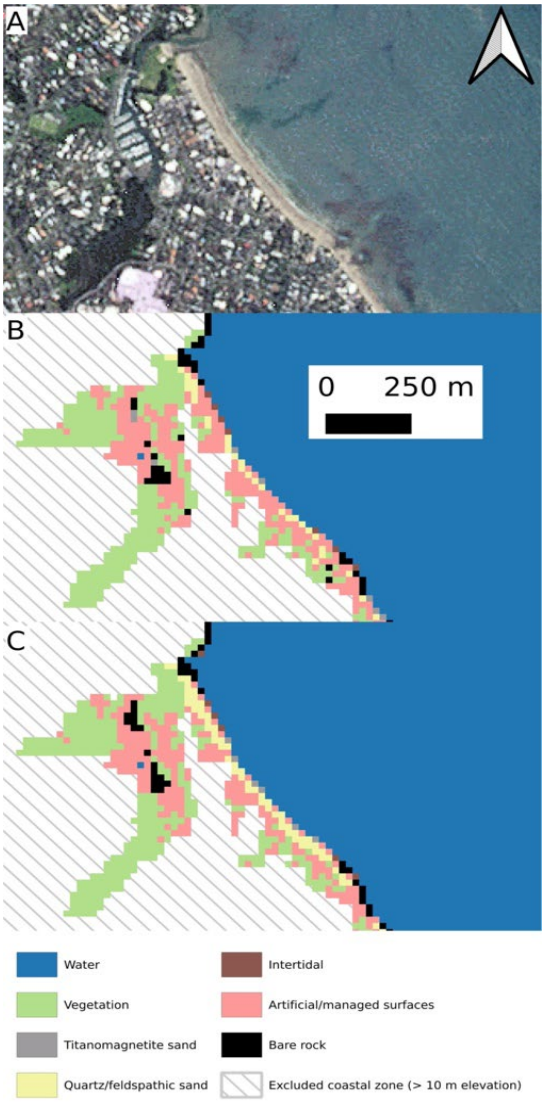

Figure 5 A. True colour image from RapidEye acquired 11/2019 of Milford beach, Auckland B. Optical classification output C. Optical/SAR classification output. Misclassification of artificial/managed surface pixels as quartz-feldspathic sand is reduced when SAR/optical data are used to train the classifier. Accurate detection is instrumental for per-pixel change detection workflows.

Whilst the fusion of SAR and optical data led to improved demarcation of these classes, misclassification was still evident in areas where development was sparse and physical characteristics between anthropogenic land cover and beaches were similar (Figure 3, D). Significant improvements were also evident in the rock coast class, despite having the lowest UA value. No omission errors and high commission errors (associated with all other classes) suggest that whilst the workflow is effective at identifying rock coast it is over-represented. Previous studies have found that the random forest algorithm can be sensitive to size and distribution of training data [24]. Area-proportional training has been found to produce best results where classes covering larger geographic areas required greater training data to be fully represented in outputs [5]. Misclassification of artificial/managed surfaces at rural remote beaches and high commission errors for rock coast suggest these classes are over-represented in the training data. Rock coast within the Auckland region covers the smallest area relative to the other thematic classes. Further work is required to assess the impact of training data on the supervised portion of the classification workflow.

Future work should investigate the use of area proportional training data. Next steps include the implementation of the workflow at the national scale to develop a baseline of land cover identification for New Zealand's coastal regions. Establishing a baseline is a step towards assessing change using EO data and can applied to both historical and future data to assess past, current, and future change [3]. In doing so, this can provide low-cost information to better inform coastal practitioners of changing coast especially in regions where other forms of data are limited or expensive to acquire.

5. Conclusions

A per-pixel classification workflow was developed with public EO data and Google Earth Engine to derive a land cover product specific to the coast in the Auckland region with high degrees of accuracy. Depositional sediment types (Titanomagnetite and Quartz-feldspathic sands) were accurately identified, alongside a variety of other land cover types at the coast. A combination of publicly available optical and SAR data produced better results than just optical data alone. Such an approach provides a low-cost method that can be implemented at the national scale. This is the initial step toward per-pixel change detection enabling better understandings of New Zealand's changing coast at macroscales.

6. Acknowledgements

This research was funded by the Resilience to Nature's Challenges National Science Challenge through the New Zealand Ministry of Business,

Innovation and Employment as part of the Coastal Programme under the 'New Zealand's Changing Coastline' project.

7. References

[1] Boak, E. H., and Turner, I. L., (2005). Shoreline Definition and Detection: A Review, Journal of Coastal Research, Vol. 21, No. 4, pp. 688–703.

[2] Breiman, L., (2001). Random Forests, Machine Learning, Vol. 45, pp. 5–32.

[3] Bunting, P., Rosenqvist, A., Lucas, R. M., Rebelo, L. M., Hilarides, L., Thomas, N., Hardy, A., Itoh, T., Shimada, M., and Finlayson, C. M., (2018). The global mangrove watch - A new 2010 global baseline of mangrove extent, Remote Sensing, Vol. 10, No. 10.

[4] Carter, L., Manighetti, B., Elliot, M., Trustrum, N., and Gomez, B., (2002). Source, sea level and circulation effects on the sediment flux to the deep ocean over the past 15 ka off eastern New Zealand, Global and Planetary Change, Vol. 33, No. 3–4, pp. 339–355.

[5] Colditz, R., (2015). An Evaluation of Different Training Sample Allocation Schemes for Discrete and Continuous Land Cover Classification Using Decision Tree-Based Algorithms, Remote Sensing, Vol. 7, No. 8, pp. 9655–9681.

[6] Farr, T. G., Rosen, P. A., Caro, E., Crippen, R., Duren, R., Hensley, S., Kobrick, M., Paller, M., Rodriguez, E., Roth, L., Seal, D., Shaffer, S., Shimada, J., Umland, J., Werner, M., Oskin, M., Burbank, D., and Alsdorf, D. E., (2007). The shuttle radar topography mission, Reviews of Geophysics, Vol. 45, No. 2, pp. 2004–2037.

[7] Feyisa, G. L., Meilby, H., Fensholt, R., and Proud, S. R., (2014). Automated Water Extraction Index: A new technique for surface water mapping using Landsat imagery, Remote Sensing of Environment, Vol. 140, pp. 23–35.

[8] Gao, B., (1996). NDWI—A normalized difference water index for remote sensing of vegetation liquid water from space, Remote Sensing of Environment, Vol. 58, No. 3, pp. 257–266.

[9] Gehrels, W. R., and Woodworth, P. L., (2013). When did modern rates of sea-level rise start?, Global and Planetary Change, Vol. 100, pp. 263–277.

[10] Gorelick, N., Hancher, M., Dixon, M., Ilyushchenko, S., Thau, D., and Moore, R., (2017). Google Earth Engine: Planetary-scale geospatial analysis for everyone, Remote Sensing of Environment, Vol. 202, pp. 18–27.

[11] Hagenaars, G., de Vries, S., Luijendijk, A. P., de Boer, W. P., and Reniers, A. J. H. M., (2018). On the accuracy of automated shoreline detection derived from satellite imagery: A case study of the sand motor mega-scale nourishment, Coastal Engineering, Vol. 133, pp. 113–125.

[12] Lawrence, J., Sullivan, F., Lash, A., Ide, G., Cameron, C., and McGlinchey, L., (2015). Adapting to changing climate risk by local government in New Zealand: institutional practice barriers and enablers, Local Environment, Vol. 20, No. 3, pp. 298–320.

[13] Lillesand, T. M., and Kiefer, R. W., (1999). Remote Sensing and Image Interpretation, John Wiley and Sons, Hoboken, 287 pp.

[14] Lu, D., and Weng, Q., (2007). A survey of image classification methods and techniques for improving classification performance, International Journal of Remote Sensing, Vol. 28, No. 5, pp. 823–870.

[15] Luijendijk, A., Hagenaars, G., Ranasinghe, R., Baart, F., Donchyts, G., and Aarninkhof, S., (2018). The State of the World's Beaches, Scientific Reports, Vol. 8, No. 6641, pp. 1–11.

[16] Murray, N. J., Phinn, S. R., DeWitt, M., Ferrari, R., Johnston, R., Lyons, M. B., Clinton, N., Thau, D., and Fuller, R. A., (2019). The global distribution and trajectory of tidal flats, Nature, Vol. 565, No. 7738. pp. 222–225.

[17] Oppenheimer, M., Glavovic, B. C., Hinkel, J., van de Wal, R., Magnan, A. K., Abd-Elgawad, A., Cai, R., Cifuentes-Jara, M., DeConto, R. M., Ghosh, T., Hay, J., Isla, F., Marzeion, B., Meyssignac, B., and Sebesvari, Z., (2019). Sea Level Rise and Implications for Low-Lying Islands, Coasts and Communities, in: Pörtner, H.-O., Roberts, D.C. , Masson-Delmotte, V., Zhai, P. M., Tignor, Poloczanska, E., Mintenbeck, K., Alegría, A., Nicolai, M., Okem, A., Petzold, J., Rama, A., Weyer N.M. (eds), IPCC Special Report on the Ocean and Cryosphere in a Changing Climate, pp. 323–411, Intergovernmental Panel on Climate Change, Geneva.

[18] Otsu, N., (1979). A Threshold Selection Method from Gray-Level Histograms, IEEE Transactions on Geoscience and Remote Sensing, Vol. 9, No. 1, pp. 62–66.

[19] Revell, D. L., Battalio, R., Spear, B., Ruggiero, P., and Vandever, J., (2011). A methodology for predicting future coastal hazards due to sea-level rise on the California Coast, Climatic Change, Vol. 109, No. 1, pp. 251–276.

[20] Vandebroek, E., Lindenbergh, R., van Leijen, F., de Schipper, M., de Vries, S., and Hanssen, R., (2017). Semi-automated monitoring of a mega-scale beach nourishment using high-resolution terraSAR-X satellite data, Remote Sensing, Vol. 9, No. 7.

[21] Vos, K., Harley, M. D., Splinter, K. D., Simmons, J. A., and Turner, I. L., (2019). Sub-annual to multi-decadal shoreline variability from publicly available satellite imagery, Coastal Engineering, Vol. 150, pp. 160–174.

[22] Xu, H., (2006). Modification of normalised difference water index (NDWI) to enhance open water features in remotely sensed imagery, International Journal of Remote Sensing, Vol. 27, No. 14, pp. 3025–3033.

[23] Xu, N., (2018). Detecting Coastline Change with All Available Landsat Data over 1986–2015: A Case Study for the State of Texas, USA, Atmosphere, Vol. 9, No. 107, pp. 1–20.